HHS Public Access

Author manuscript

J Immunol. Author manuscript; available in PMC 2017 January 01.

Published in final edited form as:

J Immunol. 2016 January 1; 196(1): 232–243. doi:10.4049/jimmunol.1402421.

Lunatic, Manic and Radical Fringe Each Promote T and B Cell Development

Yinghui Song[*,†], **Vivek Kumar**[*], **Hua-Xing Wei**, **Ju Qiu**[‡], and **Pamela Stanley**[§]

Dept. Cell Biology, Albert Einstein College of Medicine, New York, NY, 10461

Abstract

Lunatic, Manic and Radical Fringe (LFNG, MFNG and RFNG) are N-acetylglucosaminyltransferases that modify Notch receptors and regulate Notch signaling. Loss of LFNG affects thymic T cell development and LFNG and MFNG are required for marginal zone (MZ) B cell development. However, roles for MFNG and RFNG in T cell development, RFNG in B cell development, or Fringes in T and B cell activation, are not identified. Here we show that *Lfng/Mfng/Rfng* triple knockout (*Fng* tKO) mice exhibited reduced binding of DLL4 Notch ligand to CD4/CD8 double-negative (DN) T cell progenitors, and reduced expression of NOTCH1 targets Deltex1 and CD25. *Fng* tKO mice had reduced frequencies of DN1/cKit+ and DN2 T cell progenitors and CD4+CD8+ double positive (DP) T cell precursors, but increased frequencies of CD4+ and CD8+ single positive (SP) T cells in thymus. In spleen, *Fng* tKO mice had reduced frequencies of CD4+, CD8+, central memory T cells and marginal zone (MZ) B cells, and an increased frequency of effector memory T cells, neutrophils, follicular (Fo) and MZ P B cells. The *Fng* tKO phenotype was cell-autonomous and largely rescued in mice expressing one allele of a single *Fng* gene. Stimulation of *Fng* tKO splenocytes with anti-CD3/CD28 beads or lipopolysaccharide gave reduced proliferation compared to controls, and the generation of activated T cells by concanavalin A or L-PHA was also reduced in *Fng* tKO mice. Therefore, each Fringe contributes to T and B cell development, and Fringe is required for optimal in vitro stimulation of T and B cells.

Introduction

Lunatic, Manic and Radical Fringe are glycosyltransferases that transfer N-acetylglucosamine to O-linked fucose (O-fucose) present at a particular consensus site of epidermal growth factor-like (EGF) repeats (1, 2). Mammalian Fringe genes *Lfng*, *Mfng* and *Rfng* were identified based on their sequence homology to *Drosophila* Fringe (3, 4), originally identified as a gene that modifies Notch signaling (5). Subsequently, mice lacking *Lfng* were shown to have severe skeletal defects and disrupted Notch signaling during

[§]Corresponding author: pamela.stanley@einstein.yu.edu; Phone +1(718)430-3346; Fax +1(718)430-8574.

[*]These authors contributed equally

[†]Present address: Dept. Genetics, Albert Einstein College Medicine, New York, NY, 10461

[‡]Present address: Institute of Health Sciences, Shanghai Institutes for Biological Sciences, Chinese Academy of Sciences & Shanghai Jiao Tong University School of Medicine, Shanghai, 200031, China

Disclosures

The authors have no financial conflicts of interest.

somitogenesis (6, 7). The finding that Fringe modification of Notch receptors alters their binding of, and response to, Notch ligands (8–10), identified a mechanistic basis for the regulatory effects of Fringe glycosyltransferases on Notch signaling.

The first indication that Fringe could affect the regulation of T cell development was obtained when *Lfng* was mis-expressed in thymus under the control of the *lck*-proximal promoter (11). Large numbers of B cells are generated in the thymus of *lck-Lfng* transgenic mice. *Lfng* is normally expressed in CD4−CD8− double negative (DN) T cell progenitors, expressed poorly in CD4+CD8+ double positive (DP) T cell precursors, and expressed at high levels in CD4+ and CD8+ single positive (SP) T cells (12, 13). Mis-expression of *Lfng* in *lck-Lfng* DP T cell precursors leads to their increased binding to Notch ligands on stromal cells, which blocks the access of DN T cell progenitors to thymic stroma, thereby allowing the differentiation of early T cell progenitors to B cells (14). Consistent with this, inactivation of *Lfng* causes reduced competitiveness in mixed repopulation experiments, and reduced T cell development from fetal liver cells (12), or from thymocytes expressing shRNA-targeted *Lfng* (13). NOTCH1 was implicated directly as a substrate of LFNG by showing that T cell development in thymus from $Notch1^{(12f/12f)}$:*lck-Lfng* mice, in which NOTCH1 lacks the O-fucose site in the Notch ligand binding domain, is less affected by *lck-Lfng* (15). Roles for *Mfng* and *Rfng* in T cell development have not been reported, nor have roles for *Rfng* during B cell development. However, both *Lfng* and *Mfng* are important for optimal MZ B cell development in spleen (16). All three Fringe genes are expressed in DN T cell progenitors and mature T and B cells of the mouse (17–19).

In this paper, we investigate T and B cell development in mutant mice with inactivated *Fng* genes (20), including mice lacking a single *Fng* gene, all three *Fng* genes, or expressing only a single *Fng* (i. e. lacking two of the three *Fng* genes). While loss of *Lfng* may cause perinatal lethality, *Lfng* null homozygotes in a FVB/C57BL/6 mixed genetic background live for several months, although they are small, lack a tail, and are infertile (20–22). Deletion of *Mfng* or *Rfng* separately or together has no obvious effects on development or fertility (20, 23, 24). Here we show that DN T cell progenitors lacking expression of all three *Fng* genes (*Fng* tKO) had reduced binding of Notch ligand DLL4 and reduced expression of the Notch targets Deltex1 and CD25. *Fng* tKO cells had altered frequencies of several T and B cell subsets in thymus and spleen, and this phenotype was transferable by bone marrow transplantation. Mice expressing only a single allele of *Lfng, Mfng or Rfng* were rescued in the major T and B cell subset frequencies. Finally, splenic T and B cell responses to various stimulants were reduced in *Fng* tKO mice.

Materials and Methods

Mice

Mice null for *Mfng* and *Rfng* and heterozygous for *Lfng* on a mixed C57BL/6/FVB background were a kind gift of Susan Cole (University of Ohio) and are described in Moran et al. (20). The mice were intercrossed to obtained triple knockout (*Fng* tKO) mice, in which all three *Fng* genes were inactivated. They were also crossed with FVB mice to generate mice expressing all three *Fng* genes (*Fng* LMR). The latter expressed one allele of each *Fng* gene or were $Lfng^{+/+}Mfng^{+/-}Rfng^{+/-}$. *Fng* LMR and *Fng* tKO mice were also generated by

crossing *Lfng*$^{+/-}$*Mfng*$^{-/-}$*Rfng*$^{-/-}$ mice to *Fng* LMR mice. *Rfng*$^{+/-}$ mice (23) on a mixed background were obtained from the Jackson Laboratory (Bar Harbor, ME) and backcrossed for 5–6 generations to C57BL/6 mice before intercrossing. CD45.2+ C57BL/6 mice were also obtained from the Jackson Laboratory. Genotyping was performed by PCR of genomic DNA using primers that distinguish wild type and mutant alleles as described previously (20). Mice were housed in a barrier facility, allowed to eat and drink *ad libitum*, and used in experiments at 6–8 weeks of age. All experiments were performed with permission from the Albert Einstein Institutional Use and Animal Care Committee. Euthanized mice were weighed, and isolated thymus and spleen were also weighed before making single cell suspensions.

Antibodies

Except where noted, Abs and Ab conjugates to FITC, PE or allophycocyanin (APC) were from eBioscience (San Diego, CA) as follows: CD4-FITC rat IgG_{2a} clone RM4–5; CD8a–APC rat IgG_{2a} clone 53–6.7; CD25-FITC rat IgM κ clone 7D4 (BD Biosciences, San Jose, CA); CD44-Alexa Fluor^{700} rat IgG_{2b} κ clone 1M7; IgM-APC rat IgG_{2a} clone II/41; B220-Alexa Fluor^{700} rat IgG_{2a}, clone RA3–6B2; CD21-FITC rat IgG_{2b} clone 7G6 (BD Biosciences); CD23-PE rat IgG_{2a} clone B3B4; APC rat IgG_{2a} isotype; Alexa Fluor^{700} rat IgG_{2a} isotype; Alexa Fluor^{700} rat IgG_{2b} isotype; FITC rat IgG_{2b} isotype; PE rat IgG_{2a} isotype; R-Phycoerythrin AffiniPure $F(ab')_2$ Frag goat-anti-human IgG, Fcγ Frag Spec (Jackson Immunoresearch, West Grove, PA); rat-anti-mouse CD16/CD32 clone 2.4G2 (mouse Fc block; BD Biosciences); CD45.2-FITC mouse IgG_{2a} clone 104; CD45.1-PE-Cyanine 7 mouse clone A20; CD4-APC mouse clone Gk1.5; anti-CD8a–PE mouse clone 53–6.7; CD25-PerCPCy5.5 rat IgG_1κ clone PC61.5; CD44-PE clone IM7. CD117-APC rat IgG_{2b} κ clone 2B8; CD11b–FITC rat IgG_{2b} clone M1/70 (BD Biosciences); CD11c–PE hamster IgG_1 clone HL3 (BD Biosciences); Gr1-APC rat IgG_{2b} clone RB6–8C5 (BD Biosciences); Ly6G–PerCPCy5.5 rat IgG_{2a} κ clone 1A8; CD62L–perCPCy5.5 rat IgG_{2a} κ clone MEL-14; CD122-PECy7 rat IgG_{2b} κ clone TM-b1 (BD Biosciences); CD69-PE Armenian Hamster IgG clone H1.2F3; FoxP3-APC rat clone FJK-16s; antigen-purified polyclonal sheep anti-NOTCH1 (aa 19–526) AF5267 (R&D Systems, Minneapolis, MN); rabbit polyclonal IgG anti-NOTCH2 (aa 25–255) sc-5545 (Santa Cruz, Dallas, TX); Rhodamine Red-X-conjugated donkey anti-sheep IgG (Jackson Immunoresearch); anti-rabbit IgG-PE (Jackson Immunoresearch).

Flow Cytometry

Single-cell suspensions from thymus or spleen were prepared using homogenization by the insert of a 3 ml syringe and passage through a 70 μm strainer. Thymocytes were washed in cold FACS binding buffer (FBB; Hank's buffered salt solution (HBSS), 2% BSA, 0.05% sodium azide, pH 7.2–7.4), resuspended, and counted in a Coulter counter. Splenocytes were incubated in 3 ml red blood cell lysis buffer (0.15 M NH_4Cl, 10 mM $KHCO_3$, 0.1 mM EDTA, pH 7.2–7.4) for 1.5 min before adding 20 ml FBB. After centrifugation and resuspension in FBB, splenocytes were counted in a Coulter counter. For Ab binding to unfixed cells, cells were incubated with fluorochrome-conjugated Abs according to standard protocols. Briefly, 5–10 × 10^5 cells were washed with 1 ml FBB, resuspended in 90 μl FBB containing 1 μl Fc block (rat-anti-mouse CD16/CD32), and incubated for 15 min on ice. Ab

diluted in FBB (10 μl) was added and the tube incubated for 30 min at 4°C. Cells were washed twice in 1 ml FBB and transferred to a 5 ml Falcon tube in 300–500 μl FBB, to which was added 5 μl 7-actinomycin D (7-AAD, BD Biosciences) in 100 μl FBB. After 10 min on ice, cells were subjected to flow cytometry. Damaged cells that were 7-AAD+ were excluded by gating. For cells that had been fixed in 4% PBS-buffered paraformaldehyde (PFA) at room temperature for 15 min and stored at 4°C, no 7-AAD was added. For fixation followed by permeabilization, the Fixation/Permeabilization solution from eBioscience was used according to the manufacturer's instructions. For all samples, immunofluorescence was analyzed using FACSCalibur or FACScan flow cytometers (BD Biosciences), and data files were analyzed using FlowJo software (Tree Star Inc., Ashland, OR).

Isolation of DN T cell progenitors

Fresh thymocytes were resuspended in isolation buffer (PBS without cations, pH 7.2–7.4, containing 0.1% BSA and 2 mM EDTA) on ice. For CD4+ CD8+ T cell depletion, 5×10^7 thymocytes were incubated with 20 μg anti-CD4 (rat IgG_{2b} clone GK1.5; BioXCell, West Lebanon, NH) and 37.5 μg anti-CD8a (rat IgG_{2a} clone 53–6.72; BioXCell) in 5 ml isolation buffer for 20 min at 4°C with tilted rotation, centrifuged, resuspended in 5 ml isolation buffer, and incubated twice with 250 μl sheep anti-rat IgG Dynabeads (Thermo Fisher Scientific, Waltham, MA) for 30 min at 4°C with tilted rotation. After each incubation, the tube was placed in a magnet for 2 min, unbound DN T cell progenitors were combined in a new tube, centrifuged and RNA was extracted from the cell pellet with 1 ml TRIZOL® (Ambion, Carlsbad, CA) as described below.

Real-time RT-PCR

DN T cell progenitors from 5×10^7 thymocytes were pipetted vigorously in 1 ml TRIZOL® and incubated for 5 min at room temperature before adding 0.2 ml chloroform. Tubes were vortexed for 15 sec, incubated at room temperature for 2–3 min, and centrifuged at 12,000 × g for 15 min at 4°C. The aqueous phase was transferred to a fresh tube, and 0.5 ml of isopropanol was added. Samples were incubated at room temperature for 10 min. Following centrifugation at 12,000 × g for 10 min at 4°C, the RNA pellet was washed once with 1 ml 75% ethanol. Samples were vortexed and centrifuged at 7,500 × g for 5 min at 4°C. The RNA pellet was air-dried for 5–10 min and dissolved in 25–30 μl RNase-free water. RNA concentration was determined by Nanodrop and cDNA was prepared from 500 ng RNA using the Verso cDNA synthesis kit (Thermo Fisher Scientific) following the manufacturer's protocol. The product was diluted in RNase-free water to 7.5 ng/μl and 2 μl was used for qRT-PCR using the following primers:

Lfng-F: 5′-CTGCACCATTGGCTACATTG; *Lfng*-R: 5′-ATGGGTCAGCTTCCACAGAG

Mfng-F: 5'-ATGCACTGCCGACTTTTTCG; *Mfng*-R: 5'-CCTGGGTTCCGTTGGTTCAG

Rfng-F: 5'-TGCTGCTGCGTACCTGGATCTC; *Rfng*-R:5 ACAGCAGAGCAATTGGTGTTGA

Hes1-F: 5’-AAGGCAGACATTCTGGAAAT; *Hes1*-R: 5’-GTCACCTCGTTCATGCACTC

Dtx1-F: 5’-CATCAGTTCCGGCAAGAC; *Dtx1*-R: 5’ATGGTGATGCAGATGTCC

cMyc-F: 5’-AGTGCTGCATGAGGAGACAC; cMyc-R: 5’ GGTTTGCCTCTTCTCCACAG

CD25-F:5’-GGAATTGGTCTATATGCGTTGCTTA;

CD25-R:5’-CATGTCTGTTGTGGTTTGTTGCTCT

Actb-F: 5’-TTCTACAATGAGCTGCGTGTG; *Actb*-R: 5’-GGGGTGTTGAAGGTCTCAAA

Gapdh-F: 5’-AAGGTCATCCCAGAGCTGAA; *Gapdh*-R: 5’-CTGCTTCACCACCTTCTTGA

Hprt-F: 5′-GGACCTCTCGAAGTGTTGGATAC;

Hprt-R: 5′-GCTCATCTTAGGCTTTGTATTTGGCT

Notch Ligand-binding Assay

Soluble Notch ligands DLL4-Fc, DLL1-Fc, JAG1-Fc and Fc control were prepared from HEK-293T cells as described previously (25). JAG2-Fc was purchased from R&D Systems. Single-cell suspensions from thymus were washed in ligand binding buffer (LBB; HBSS pH 7.4, 1 mM $CaCl_2$, 1% (w/v) BSA, 0.05% NaN_3) and fixed in PBS-buffered 4% paraformaldehyde for 15 min at room temperature, washed twice with LBB and stored in LBB at 4°C. Fixed thymocytes were washed with LBB and 3×10^6 cells were incubated with FcR blocking solution (rat-anti-mouse CD16/CD32) on ice for 15 min. Thereafter the cells were incubated in 100 μl of LBB containing anti-CD4-FITC (1:200), anti-CD8a–APC (1:200) and 500–750 ng DLL1-Fc, DLL4-Fc, JAG1-Fc, JAG2-Fc or Fc. After incubation at 4°C for 1 hour, cells were washed twice with 0.5 ml of LBB and incubated with anti-IgG-PE (Fc-specific) Ab (1:100) at 4°C for 30 min. The cells were then washed twice with 1 ml of LBB and analyzed in a FACSCalibur flow cytometer (BD Biosciences). For detection of NOTCH1 and NOTCH2 at the cell surface, fixed thymocytes were incubated with FcR block rat-anti-mouse CD16/CD32 (1:100) followed by CD4-FITC mAb (1:200), CD8a–APC mAb (1:200), sheep anti-mouse NOTCH1 Ab (1:50) or rabbit anti-human NOTCH2 Ab (1:100) at 4°C for 1 h, washed and incubated with rhodamine Red-X-conjugated donkey anti-sheep IgG (1:100) or anti-rabbit IgG-PE (1:100) at 4°C for 30 min. Cells were washed twice with 1 ml of LBB and analyzed using a FACSCalibur flow cytometer.

Bone marrow transplantation

Cell suspensions were made from bone marrow flushed from the femur of 7–8 week *Fng* LMR and *Fng* tKO mice into 5 ml cold HBSS, centrifuged and resuspended in RBC lysis buffer. After 1.5 min on ice, 10 ml HBSS was added, the cells were washed 3 times in HBSS and counted. *Fng* LMR, *Fng* tKO and a 1:1 mix (3×10^6 cells total for each sample) were injected retro-orbitally in 50 μl HBSS into CD45.2+ C57BL/6 lethally-irradiated recipients. Gamma-irradiation of 500 rads per recipient mouse was given twice, with a 16 h

interval. After 6 weeks, mice were euthanized, thymus and spleen were weighed, and thymocytes and splenocytes were analyzed for T and B cell subsets by flow cytometry after gating to remove damaged cells (7-AAD-positive), and subsequently on donor-derived cells that were double positive for staining with antibodies CD45.1-PE-Cyanine 7 and CD45.2-FITC.

Lymphocyte Proliferation Assay

Whole splenocytes (10^7 cells/ml) were incubated in 10 μM carboxyfluorescein diacetate succinimidyl ester (CFSE; Molecular Probes Inc., Eugene, OR) in PBS containing 5% heat-inactivated FBS for 10 min at 37°C. Uptake was inhibited by the addition of two volumes of ice-cold complete RPMI-1640 medium (RPMI-1640 containing 10% heat-inactivated FBS and 1% penicillin/streptomycin), and the cells were incubated on ice for 5 min. Cells were then washed twice in complete RPMI-1640 medium and resuspended to the desired concentration in complete RPMI-1640 medium. Fresh CFSE-labeled splenocytes were cultured at 10^6 cells/per well in a 24-well plate in 1 ml complete RPMI 1640 medium. T cells were stimulated by the addition of pre-washed CD3/CD28 Dynabeads (Thermo Fisher Scientific) at 25 μl/ml and rIL2 (PeproTech, Rocky Hill, NJ) at 5 ng/ml. B cells were stimulated with lipopolysaccharide (LPS) at 15 μg/ml (E.coli, serotype 055:B5 Sigma-Aldrich, St. Louis, MO). Plates were incubated in a humidified atmosphere of 5% CO_2 at 37°C. After 3 days, cells were harvested, incubated with fluorochrome-conjugated anti-CD4 (1:200) and anti-CD8a (1:200) or anti-B220 (1:100) antibodies, followed by the addition of 7-amino-actinomycinD (7-AAD; 1:20), and analyzed by flow cytometry. FlowJo algorithms were used to quantitate the CFSE profiles of viable (7-AAD negative) T or B cell populations.

T cell activation assay

T cell activation in response to concanavalin A (Con A; Pharmacia, Uppsala, Sweden) or *Phaseolus vulgaris* leukoagglutinin (L-PHA; Vector Labs, Burlingame, CA) were investigated by expression of CD69 using flow cytometry. Fresh splenocytes were washed twice in complete RPMI-1640 medium, counted, and added to 24-well culture plates at 10^6 cells per well. Splenocytes were stimulated by the addition of Con A (5 μg/ml) or L-PHA (2 μg/ml) added to duplicate wells in a final volume of 1 ml. The concentrations of Con A and L-PHA that induced maximal cell proliferation were determined in preliminary experiments. After 20 h at 37°C in a humidified atmosphere of 5% CO2, cells were harvested, washed with FBB and incubated with fluorochrome-conjugated anti-CD4 (1:200), anti-CD8a (1:200) and anti-CD69 (1:80) Abs, followed by the addition of 7-AAD (1:20). Analysis by flow cytometry was performed to determine CD69 expression on 7-AAD-negative $CD4^+$ and $CD8^+$ T cells.

Data analysis

Comparisons are presented as mean ± SEM. Significance was determined by two-tailed unpaired, parametric, Student's *t* test analysis (unless otherwise noted), using Prism software.

Results

T and B cell subsets in mice lacking a single Fng gene

Mice lacking a single *Fng* activity were compared for T and B cell development. *Lfng* mutant mice are viable on a background including C57BL/6 and FVB/NJ (20). *Lfng*$^{-/-}$ mice (FVB/C56BL/6) of 7–8 weeks had reduced body, thymus and spleen weights compared to *Fng* LMR, *Mfng*$^{-/-}$ or *Rfng*$^{-/-}$ mice (Supplemental Fig. 1), and absolute numbers of thymocytes and splenocytes were equivalently reduced. However, the ratio of thymocytes and splenocytes to body or organ weight were similar in all *Fng* mutant mice and controls. Therefore, the frequencies of different T, B and myeloid subsets in thymocyte or splenocyte populations were determined. T cell subsets were determined using antibodies against CD4, CD8a, CD44 and CD25; B cell subsets using antibodies against B220, CD21, CD23 and IgM; myeloid cells using antibodies against Gr1, CD11b and CD11c; and Tregs using antibodies against CD4 and FoxP3. No significant differences were observed between controls and single *Fng* knockout mice in the relative proportions of DN or DP T cell precursors, or CD4+ or CD8+ SP T cells in thymus (Supplemental Fig. 1). There were only minor populations of B220+, Tregs or myeloid cells in thymus, and they were similar in frequency to controls (not shown). In spleen, the proportions of CD4+ and CD8+ T cells, and B220+ cells (Supplemental Fig. 1), and myeloid cell subsets (not shown) were similar in single *Fng* knockout and *Fng* LMR mice. To determine if differences due to the absence of *Rfng* could be detected in a more homogeneous genetic background, *Rfng*$^{-/-}$ mice on a mixed 129Sv/C57BL/6 background were backcrossed to C57BL/6 for 5–6 generations and wild type and heterozygous mutant mice were compared to homozygous mutant littermates. Only minor variations in the proportions of T and B cell subsets were observed when mice were compared based on gender (Supplemental Fig. 2). Therefore, we focused on mice in which two *Fng* genes, or all three *Fng* genes were inactivated.

Notch Ligand Binding to DN T cell progenitors from Fng tKO mice

Lfng is well expressed in DN T cell progenitors but poorly expressed in DP T cell precursors that make up the majority of the thymocyte population (12, 13). Therefore, Notch ligand binding was examined using DN T cell progenitors. Thymocytes from 6–8 week *Fng* LMR and *Fng* tKO mice were fixed and incubated with CD4-FITC and CD8a–APC mAbs, along with Notch ligand-Fc or Fc control. Notch ligand binding was determined on DN T cell progenitors using anti-Fc-PE. Consistent with previous reports (26), *Fng* LMR DN T cell progenitors bound DLL4-Fc (Fig. 1A) better than DLL1-Fc (Fig. 1B). However, *Fng* tKO DN T cell progenitors exhibited markedly reduced binding of DLL4-Fc (Fig. 1A). DN T cell progenitors from *Fng* dKO mice expressing only *Mfng* or only *Rfng* were partially rescued for DLL4-Fc binding (Table I). Cell surface expression of NOTCH1 and NOTCH2 was similar in DN T cell progenitors from *Fng* LMR and *Fng* tKO mice (Supplemental Fig. 3), indicating that reduced DLL4-Fc binding primarily reflects reduced interactions with Notch receptors lacking Fringe modification. Therefore, all three Fringe activities contributed to DLL4-Fc binding to DN T cell progenitors. The absence of Fringe might be expected to enhance the binding of Notch ligands JAG1 and JAG2 as Fringe may inhibit Jagged ligand binding (25, 27), but JAG1-Fc and JAG2-Fc bound similarly to DN T cell progenitors from controls and mice lacking all three Fringe activities (Fig. 1C and 1D).

Expression of Fringe and Notch Target Genes in DN T Cell Progenitors

The expression of each Fringe gene during T cell development in C57BL/6 mice was extracted from published microarray data (Supplemental Fig. 4). The relative expression of *Lfng* and *Mfng* does not change significantly through early T cell progenitor development, is reduced in DP T cell precursors, and increases markedly in CD4+ and CD8+ SP T cells. By contrast, *Rfng* expression is relatively high in ETP progenitors, reduced in DN1 and DN2 T cells and equivalently high in DN4, DP, CD4+ and CD8+ SP T cells. The expression of Fringe and Notch target genes in DN T cell progenitors from mice expressing all *Fng* genes (LMR), a single *Fng* gene (L, M or R) or no *Fng* gene (tKO) was examined by qRT-PCR. *Fng* expression correlated directly with genotype as expected (Fig. 2A, 2B, 2C). Importantly, there was no compensatory increase in expression when any combination of two *Fng* genes was deleted. Initial experiments to examine Notch target gene expression in cDNA from *Fng* LMR and *Fng* tKO mice (n=3–6) revealed no change in relative expression compared to *Actb* of *Hes1*, *Hes5* or *Dtx2* transcripts, a reduction in CD25 to 48±1% (n=3 experiments; $p<0.0003$) of *Fng* LMR, and a significant reduction in *Dtx1* transcripts with two primer sets to 41±0.8% (n=6 experiments; $p<0.0001$). Data from a more recent cohort of mice (Fig. 2) showed equivalent relative expression of *Hes1* and cMyc and significantly reduced expression of *Dtx1* in *Fng* tKO DN T cells, compared to the combined average expression of *Actb*, *Hprt* and *Gapdh* (Fig. 2D, 2E and 2F). However, the expression of CD25 transcripts was not reduced in DN T cells from mice expressing a single Fringe, nor in *Fng* tKO DN T cells (data not shown). Therefore, we examined CD25 expression level by analyzing flow cytometry data from all cohorts. The MFI for CD25 was markedly reduced in *Fng* tKO compared to *Fng* LMR DN T cells, and was also significantly reduced in mice expressing only *Rfng* or *Mfng* (Fig. 2G). Thus, the expression of both CD25 and *Dtx1* Notch targets was consistently reduced in the absence of Fringe. Expression of a single *Fng* rescued *Dtx1* transcript levels, but only a single *Lfng* substantially rescued CD25 expression at the cell surface.

T Cell Development in Thymus of Fng tKO Mice

Fng tKO mice had a small thymus compared to *Fng* LMR mice and mice lacking only *Lfng* (*Mfng* and *Rfng* heterozygous, designated MR), but not significantly different from mice lacking both *Lfng* and *Mfng* (designated R), or both *Lfng* and *Rfng* (designated M) (Fig. 3A). Thymocyte numbers gave a similar result but were more variable (Fig. 3B). Thus *Mfng* or *Rfng* alone could not substitute for *Lfng* in the development of the thymus. However, the ratio of both thymus/body weight and the number of thymocytes/thymus weight were similar across all *Fng* mutant mice. Therefore, frequencies rather than absolute numbers of T, B and myeloid cell subsets were compared. In *Fng* tKO thymus, the frequency of DP T cell precursors decreased slightly, whereas the frequencies of CD4+ and CD8+ SP T cells were increased (Fig. 3C and 3D). When DN T cell progenitor subsets were examined using antibodies to cKit/CD117, CD44 and CD25, the proportions of DN1/cKit+ and DN2 T cell progenitors were reduced in *Fng* tKO thymus (Fig. 4). Interestingly, the proportion of B220+ B cells in the thymus was not increased in *Fng* tKO mice (0.65 ± 0.1%, n=7) compared to *Fng* LMR mice (0.62 ± 0.19%, n=3), as occurs when Notch signaling is blocked or *Lfng* is misexpressed (26). *Fng* LMR and *Fng* tKO thymocytes also contained

similarly low proportions of Treg and myeloid cells expressing Gr1, CD11b, or CD11c (data not shown).

T and B Cells in Spleen of Fng tKO Mice

Mice expressing only *Mfng*, only *Rfng*, or both, and *Fng* tKO mice had a smaller spleen by weight (Fig. 5A) and fewer splenocytes (Fig. 5B) than *Fng* LMR control mice. However, the normalized number of splenocytes to spleen weight was similar in *Fng* mutant and *Fng* LMR mice. The proportion of B220+ B cells was unchanged (∼50% of the CD4−CD8− splenocytes) by the absence of Fringe (Fig. 5C), but the proportions of both $CD4^+$ and $CD8^+$ T cells were decreased in *Fng* tKO spleen (Fig. 5D). Effector and memory T cell populations were also affected by the absence of Fringe. CD4+ and CD8+ splenocytes examined for CD44 and CD62L expression showed a reduction in the proportion of naïve T cells ($CD44^{lo}CD62L^{hi}$) as expected, an increase in T effector memory cells ($CD44^{hi}CD62L^{lo}$), and a reduction in central memory T cells ($CD44^{hi}CD62L^{hi}$) in *Fng* tKO mice (Fig. 6A and 6B). CD8+ splenocytes gave a similar result when CD44 and CD122 expression were compared – a reduced proportion of $CD44^{hi}CD122^{hi}$ central memory T cells, and an increased proportion of $CD44^{hi}CD122^{lo}$ effector memory T cells (Fig. 6C). For B220+ cells, the frequency of follicular B (Fo B) cells was increased (Fig. 7A and 7B) while the proportion of MZ B cells was decreased in *Fng* tKO splenocytes (Fig. 7C and 7D). MZ P cell frequency was concomitantly increased (Fig. 7C). These results are consistent with evidence that *Lfng* and *Mfng* are both required for optimal MZ B cell development (16). Finally, in all forward (FSC) versus side scatter (SSC) profiles of fresh or fixed splenocytes (including cells stored for several months at 4°C), we observed an increased population of granulated cells (SSC^{hi}) in *Fng* tKO spleen. Initial investigations revealed an increased frequency of Ly6G+ cells in *Fng* tKO splenocytes. Subsequently, we determined that Gr1+Ly6G+ neutrophils were significantly increased in splenocytes from *Fng* tKO compared to *Fng* LMR mice (Fig. 7E and 7F), a phenotype consistent with reduced Notch signaling in bone marrow (28).

The Fng tKO phenotype is transferable

To determine if the *Fng* tKO phenotype is cell-autonomous, bone marrow transplantation experiments were performed. Two of three experiments gave >35% reconstitution of donor bone marrow. In one experiment donor reconstitution was ∼40% for thymus and spleen, and there were no significant differences between T and B cell subset frequencies for cells derived from *Fng* tKO versus *Fng* LMR bone marrow. However, in the experiment in which *Fng* tKO and *Fng* LMR control donor cells made up 74%-88% of host thymocytes and 64%-74% of host splenocytes, a cell-autonomous effect for *Fng* tKO recipients was observed (Fig. 8). Thus, thymus weight and DP T cell precursor frequency were reduced in recipients of *Fng* tKO versus *Fng* LMR bone marrow, or an equal mixture of *Fng* LMR and *Fng* tKO bone marrow (Fig. 8A). In addition, frequencies of donor-derived CD4+ and CD8+ SP T cells were increased in thymus (Fig. 8A), as observed in *Fng* tKO thymus (Fig. 3). In spleen, reconstitution from *Fng* tKO bone marrow resulted in a significant decrease in the frequencies of CD4+ and CD8+ T cells (Fig. 8B), as observed in *Fng* tKO spleen (Fig. 5). Importantly, the proportion of each T cell subset was similar in thymus and spleen from mice that received *Fng* LMR cells or the 1:1 mix of *Fng* LMR and *Fng* tKO mice, indicating

that the differential production of T cells from *Fng* tKO bone marrow was overcome by co-injection with *Fng* LMR bone marrow.

T and B Cell Development in Mice Expressing a Single Fng Gene

To identify roles for individual Fringe activities, we analyzed *Fng* dKO mice in which only one *Fng* gene was active. A single allele of either *Mfng* or *Rfng* did not rescue the reduced thymocyte and splenocyte numbers observed in *Fng* tKO mice (Figs. 3 and 5), so T and B cell subset frequencies were compared. There were no significant differences in the frequencies of DN, DP, or SP T cells in thymus of mice expressing a single Fringe versus *Fng* LMR control mice (Fig. 9A). Therefore each Fringe, acting alone, could restore the reduced proportion of DP T cell precursors, and did not exhibit the increased proportions of CD4+ and CD8+ T cells observed in *Fng* tKO thymus (Fig. 3).

In spleen, the percentage of CD4+ T cells from mice expressing only *Rfng* or *Lfng* was similar to *Fng* LMR mice (Fig. 9B), demonstrating rescue compared to *Fng* tKO mice (Fig. 5D). However, mice expressing only *Mfng* were only partially rescued (Fig. 9B). By contrast, for the CD8+ T cell subset in spleen, mice expressing only *Mfng* or only *Rfng* were rescued, but mice expressing only *Lfng* were not fully rescued (Fig. 9B). The proportion of B220+ and Fo B splenocytes was not changed in mice expressing a single Fringe gene compared to F*ng* LMR mice (Fig. 9B). However, MZ B cell frequencies in spleen from mice expressing only one allele of *Mfng* or *Rfng* were significantly reduced, whereas mice expressing only *Lfng* were similar to *Fng* LMR mice (Fig. 9B). These results show that each Fringe enzyme was largely sufficient, in the absence of the other two Fringes, to support T cell development in thymus and spleen, although MZ B cell production was not optimal in mice expressing only *Mfng* or only *Rfng*. Rescue of the *Fng* tKO T cell phenotype was not expected for *Rfng*. To demonstrate functional effects of *Rfng* more clearly, T cell subsets from mice expressing one allele of *Rfng* were compared to *Fng* tKO (Fig. 10). It is apparent that *Rfng* was able to restore T cell subset frequencies to control levels in both thymus and spleen.

T and B cell activation were reduced in the absence of Fringe

T and B cell activation were investigated by stimulation with anti-CD3/CD28 Dynabeads and IL 2, or LPS, respectively. Stimulation of splenocytes with anti-CD3/CD28 Dynabeads and IL-2 showed that proliferation was reduced in both CD4+ and CD8+ T cell subsets from *Fng* tKO spleen (Fig. 11A and 11B). Stimulation of splenocytes by LPS revealed that B cells lacking Fringe also proliferated less well (Fig. 11C). Stimulation by the lectins Con A or L-PHA caused expression of CD69 in most CD4+ and CD8+ *Fng* LMR splenic T cells. However, the number of activated T cells was reduced following Con A or L-PHA stimulation of T cells lacking Fringe, particularly in the CD4+ subset (Fig. 11D and 11E).

Discussion

Here we show that *Mfng* and *Rfng* are required for optimal T and B cell development. While *Lfng* plays a major role in promoting general development of thymus and spleen as well as T and B cell development, we found quite unexpectedly that when *Lfng* was absent, a single

allele of *Mfng* or *Rfng* supported the development of normal, or nearly normal proportions, of most T and B cell subsets. When all three *Fng* genes were inactivated, reduced Notch signaling and Notch ligand binding were evident in thymic DN T cell progenitors. It is of interest that the large reduction in DLL4-Fc binding to DN T cells was reflected in only a modest reduction in Notch signaling. This is presumably because DLL4-Fc soluble ligand binds weakly to NOTCH receptors, and may be more Fringe-dependent, than membrane-bound DLL4, which must signal quite well, but clearly not optimally, in the absence of Fringe. Thus, the proportions of thymus ETP and DN2 T cell progenitors and DP T cell precursors were reduced. However, the frequencies of CD4+ and CD8+ SP T cells in thymus were slightly increased in mice lacking the three Fringe activities. These effects were also observed when *Fng* tKO bone marrow cells were transferred to irradiated hosts, showing that the effects of *Fng* were cell autonomous, as observed in other contexts (26).

The increased frequency of CD4+ and CD8+ SP T cells in *Fng* tKO thymus is intriguing. Potential and non-exclusive explanations include: 1) SP T cells lacking all Fringe activities emigrate from the thymus at a slower rate compared to mice expressing *Fng*; 2) the transition from DP T cell precursors to SP T cells occurs at a slightly faster rate in *Fng* tKO thymus compared to control thymus, as observed previously in *Notch1*$^{12f/12f}$ thymus in which Notch1 signaling is reduced (29); and 3) SP T cells undergo clonal deletion at a slower rate in *Fng* tKO thymus compared to control thymus. In *Fng* tKO mice and recipients of *Fng* tKO bone marrow, the numbers of CD4+ and CD8+ T cells in spleen were reduced, suggesting they are either preferentially retained in the thymus, lost during passage to spleen, or have reduced survival upon their arrival in spleen.

Whatever cellular mechanisms are responsible for the phenotype of *Fng* tKO mice, it is apparent that expression of a single *Fng* gene is sufficient to support the generation of normal proportions of the major T and B cell populations. However, a single allele of *Rfng* or *Mfng* is not sufficient to generate normal levels of spleen MZ B cells. Thus, it is probable that mice expressing only *Rfng* or *Mfng* would exhibit defective innate immunity, and potentially altered adaptive immunity to certain pathogens (30, 31). In fact, since we show here that splenic T and B cells from mice lacking all Fringe activities exhibited a reduced frequency of central memory T cells, and reduced responses to stimulation by anti-CD3/CD28 beads, LPS, Con A and L-PHA, it can be expected that immunological functions will be uncovered for potentially each mammalian Fringe when mutant mice are subjected to immunological challenges. For example, the *Rfng* gene is upregulated, whereas *Lfng* and *Mfng* genes are downregulated in naïve CD4+ T cells in lungs of asthmatic rats (32). Knockdown of *Rfng* or overexpression of *Mfng* or *Lfng* in CD4+ naïve T cells from asthmatic lung reduces their production of Th2 cytokines, and increases their production of Th1 cytokines. Some functional consequences of loss of *Mfng* have also been noted in B cell and macrophage responses in a general survey of a small cohort of mutant mice (33). In that study, B cells from *Mfng*$^{-/-}$ mice exhibited increased proliferation following stimulation with anti-IgM, and responded with infiltration of fewer macrophages to intraperitoneal stimulation by thioglycollate. It might also be expected that mammalian Fringe activities have roles in certain lymphomas or leukemias. Thus, *Lfng* loss in mouse prostate leads to prostatic intraepithelial neoplasia (34), and *Lfng* loss in mouse breast was found to co-

operate with amplification of the Met/Caveolin gene to promote basal-like breast cancer (35).

Investigations into the mechanism by which Fringe affects Notch signaling have been performed in co-cultures using cells expressing Notch ligands (36, 37). Interestingly, both groups show that DLL4 and JAG2 induce Notch signaling that promotes T cell development. Both groups also found increased Notch signaling and T cell development following the introduction of *Lfng* into fetal liver cells or human hematopoietic stem cells, respectively. Structural and *in vitro* Notch ligand binding and signaling experiments (38) (and references therein), as well as the data reported in this manuscript, support the interpretation that the addition of GlcNAc by Fringe to Notch in signal-receiving T and B cells, increases Notch ligand binding and thereby Notch signaling, which affects the differentiation of T and B cells in thymus and spleen, and the functions of mature T and B cells in response to stimulation.

Supplementary Material

Refer to Web version on PubMed Central for supplementary material.

Acknowledgements

The authors thank Susan Cole (University of Ohio) for providing mice carrying mutant alleles of *Lfng*, *Mfng* and *Rfng*, and Cynthia Guidos (University of Toronto and Hospital for Sick Children) for helpful comments. The authors are most grateful to Wen Dong, Huimin Shang and Subha Sundaram for technical assistance.

This work was supported by grants from the National Institutes of Heath to PS (NCI RO1 95022 and NIGMS RO1 GM106417), and partial support was provided by the Albert Einstein Cancer Center (NCI grant PO1 13333).

References

1. Rampal R, Li AS, Moloney DJ, Georgiou SA, Luther KB, Nita-Lazar A, Haltiwanger RS. Lunatic fringe, manic fringe, and radical fringe recognize similar specificity determinants in O-fucosylated epidermal growth factor-like repeats. J Biol Chem. 2005; 280:42454–42463. [PubMed: 16221665]
2. Rana NA, Haltiwanger RS. Fringe benefits: functional and structural impacts of O-glycosylation on the extracellular domain of Notch receptors. Curr Opin Struct Biol. 2011; 21:583–589. [PubMed: 21924891]
3. Johnston SH, Rauskolb C, Wilson R, Prabhakaran B, Irvine KD, Vogt TF. A family of mammalian Fringe genes implicated in boundary determination and the Notch pathway. Development. 1997; 124:2245–2254. [PubMed: 9187150]
4. Cohen B, Bashirullah A, Dagnino L, Campbell C, Fisher WW, Leow CC, Whiting E, Ryan D, Zinyk D, Boulianne G, Hui CC, Gallie B, Phillips RA, Lipshitz HD, Egan SE. Fringe boundaries coincide with Notch-dependent patterning centres in mammals and alter Notch-dependent development in Drosophila. Nat Genet. 1997; 16:283–288. [PubMed: 9207795]
5. Irvine KD, Wieschaus E. fringe, a Boundary-specific signaling molecule, mediates interactions between dorsal and ventral cells during Drosophila wing development. Cell. 1994; 79:595–606. [PubMed: 7954826]
6. Evrard YA, Lun Y, Aulehla A, Gan L, Johnson RL. lunatic fringe is an essential mediator of somite segmentation and patterning. Nature. 1998; 394:377–381. [PubMed: 9690473]
7. Zhang N, Gridley T. Defects in somite formation in lunatic fringe-deficient mice. Nature. 1998; 394:374–377. [PubMed: 9690472]

8. Moloney DJ, Panin VM, Johnston SH, Chen J, Shao L, Wilson R, Wang Y, Stanley P, Irvine KD, Haltiwanger RS, Vogt TF. Fringe is a glycosyltransferase that modifies Notch. Nature. 2000; 406:369–375. [PubMed: 10935626]
9. Bruckner K, Perez L, Clausen H, Cohen S. Glycosyltransferase activity of Fringe modulates Notch-Delta interactions. Nature. 2000; 406:411–415. [PubMed: 10935637]
10. Hicks C, Johnston SH, diSibio G, Collazo A, Vogt TF, Weinmaster G. Fringe differentially modulates Jagged1 and Delta1 signalling through Notch1 and Notch2. Nat Cell Biol. 2000; 2:515–520. [PubMed: 10934472]
11. Koch U, Lacombe TA, Holland D, Bowman JL, Cohen BL, Egan SE, Guidos CJ. Subversion of the T/B lineage decision in the thymus by lunatic fringe-mediated inhibition of Notch-1. Immunity. 2001; 15:225–236. [PubMed: 11520458]
12. Visan I, Tan JB, Yuan JS, Harper JA, Koch U, Guidos CJ. Regulation of T lymphopoiesis by Notch1 and Lunatic fringe-mediated competition for intrathymic niches. Nat Immunol. 2006; 7:634–643. [PubMed: 16699526]
13. Tsukumo S, Hirose K, Maekawa Y, Kishihara K, Yasutomo K. Lunatic fringe controls T cell differentiation through modulating notch signaling. J Immunol. 2006; 177:8365–8371. [PubMed: 17142733]
14. Visan I, Yuan JS, Tan JB, Cretegny K, Guidos CJ. Regulation of intrathymic T-cell development by Lunatic Fringe- Notch1 interactions. Immunol Rev. 2006; 209:76–94. [PubMed: 16448535]
15. Visan I, Yuan JS, Liu Y, Stanley P, Guidos CJ. Lunatic fringe enhances competition for delta-like Notch ligands but does not overcome defective pre-TCR signaling during thymocyte beta-selection in vivo. J Immunol. 2010; 185:4609–4617. [PubMed: 20844195]
16. Tan JB, Xu K, Cretegny K, Visan I, Yuan JS, Egan SE, Guidos CJ. Lunatic and manic fringe cooperatively enhance marginal zone B cell precursor competition for delta-like 1 in splenic endothelial niches. Immunity. 2009; 30:254–263. [PubMed: 19217325]
17. Wu C, Macleod I, Su AI. BioGPS and MyGene.info: organizing online, gene-centric information. Nucleic Acids Res. 2013; 41:561–565.
18. Rothenberg EV. Epigenetic mechanisms and developmental choice hierarchies in T-lymphocyte development. Briefings in functional genomics. 2013; 12:512–524. [PubMed: 23922132]
19. Rothenberg EV, Champhekar A, Damle S, Del Real MM, Kueh HY, Li L, Yui MA. Transcriptional Establishment of Cell-Type Identity: Dynamics and Causal Mechanisms of T-Cell Lineage Commitment. Cold Spring Harb Symp Quant Biol. 2013; 78:31–41. [PubMed: 24135716]
20. Moran JL, Shifley ET, Levorse JM, Mani S, Ostmann K, Perez-Balaguer A, Walker DM, Vogt TF, Cole SE. Manic fringe is not required for embryonic development, and fringe family members do not exhibit redundant functions in the axial skeleton, limb, or hindbrain. Dev Dyn. 2009; 238:1803–1812. [PubMed: 19479951]
21. Hahn KL, Johnson J, Beres BJ, Howard S, Wilson-Rawls J. Lunatic fringe null female mice are infertile due to defects in meiotic maturation. Development. 2005; 132:817–828. [PubMed: 15659488]
22. Hahn KL, Beres B, Rowton MJ, Skinner MK, Chang Y, Rawls A, Wilson-Rawls J. A deficiency of lunatic fringe is associated with cystic dilation of the rete testis. Reproduction. 2009; 137:79–93. [PubMed: 18801836]
23. Zhang N, Norton CR, Gridley T. Segmentation defects of Notch pathway mutants and absence of a synergistic phenotype in lunatic fringe/radical fringe double mutant mice. Genesis. 2002; 33:21–28. [PubMed: 12001066]
24. Svensson P, Bergqvist I, Norlin S, Edlund H. MFng is dispensable for mouse pancreas development and function. Mol Cell Biol. 2009; 29:2129–2138. [PubMed: 19223466]
25. Stahl M, Uemura K, Ge C, Shi S, Tashima Y, Stanley P. Roles of Pofut1 and O-fucose in mammalian Notch signaling. J Biol Chem. 2008; 283:13638–13651. [PubMed: 18347015]
26. Yuan JS, Kousis PC, Suliman S, Visan I, Guidos CJ. Functions of notch signaling in the immune system: consensus and controversies. Annu Rev Immunol. 2010; 28:343–365. [PubMed: 20192807]

27. Yang LT, Nichols JT, Yao C, Manilay JO, Robey EA, Weinmaster G. Fringe glycosyltransferases differentially modulate Notch1 proteolysis induced by Delta1 and Jagged1. Mol Biol Cell. 2005; 16:927–942. [PubMed: 15574878]
28. Yao D, Huang Y, Huang X, Wang W, Yan Q, Wei L, Xin W, Gerson S, Stanley P, Lowe JB, Zhou L. Protein O-fucosyltransferase 1 (Pofut1) regulates lymphoid and myeloid homeostasis through modulation of Notch receptor ligand interactions. Blood. 2011; 117:5652–5662. [PubMed: 21464368]
29. Ge C, Stanley P. The O-fucose glycan in the ligand-binding domain of Notch1 regulates embryogenesis and T cell development. Proc Natl Acad Sci U S A. 2008; 105:1539–1544. [PubMed: 18227520]
30. Lopes-Carvalho T, Foote J, Kearney JF. Marginal zone B cells in lymphocyte activation and regulation. Curr Opin Immunol. 2005; 17:244–250. [PubMed: 15886113]
31. Cerutti A, Cols M, Puga I. Marginal zone B cells: virtues of innate-like antibody-producing lymphocytes. Nat Rev Immunol. 2013; 13:118–132. [PubMed: 23348416]
32. Gu W, Xu W, Ding T, Guo X. Fringe controls naive CD4(+)T cells differentiation through modulating notch signaling in asthmatic rat models. PLoS One. 2012; 7:47288.
33. Orr SL, Le D, Long JM, Sobieszczuk P, Ma B, Tian H, Fang X, Paulson JC, Marth JD, Varki N. A phenotype survey of 36 mutant mouse strains with gene-targeted defects in glycosyltransferases or glycan-binding proteins. Glycobiology. 2013; 23:363–380. [PubMed: 23118208]
34. Zhang S, Chung WC, Wu G, Egan SE, Xu K. Tumor-suppressive activity of Lunatic Fringe in prostate through differential modulation of Notch receptor activation. Neoplasia. 2014; 16:158–167. [PubMed: 24709423]
35. Xu K, Usary J, Kousis PC, Prat A, Wang DY, Adams JR, Wang W, Loch AJ, Deng T, Zhao W, Cardiff RD, Yoon K, Gaiano N, Ling V, Beyene J, Zacksenhaus E, Gridley T, Leong WL, Guidos CJ, Perou CM, Egan SE. Lunatic fringe deficiency cooperates with the Met/Caveolin gene amplicon to induce basal-like breast cancer. Cancer Cell. 2012; 21:626–641. [PubMed: 22624713]
36. Abe N, Hozumi K, Hirano K, Yagita H, Habu S. Notch ligands transduce different magnitudes of signaling critical for determination of T-cell fate. Eur J Immunol. 2010; 40:2608–2617. [PubMed: 20602435]
37. Van de Walle I, De Smet G, Gartner M, De Smedt M, Waegemans E, Vandekerckhove B, Leclercq G, Plum J, Aster JC, Bernstein ID, Guidos CJ, Kyewski B, Taghon T. Jagged2 acts as a Delta-like Notch ligand during early hematopoietic cell fate decisions. Blood. 2011; 117:4449–4459. [PubMed: 21372153]
38. Taylor P, Takeuchi H, Sheppard D, Chillakuri C, Lea SM, Haltiwanger RS, Handford PA. Fringe-mediated extension of O-linked fucose in the ligand-binding region of Notch1 increases binding to mammalian Notch ligands. Proc Natl Acad Sci U S A. 2014; 111:7290–7295. [PubMed: 24803430]

Abbreviations

Con A	Concanavalin A
L-PHA	leukoagglutinin from *Phaseolus vulgaris*
EGF	EGF-like repeat
ECD	extracellular domain
LBB	ligand binding buffer
HBSS	Hank’s balanced salt solution
FBB	FACS binding buffer

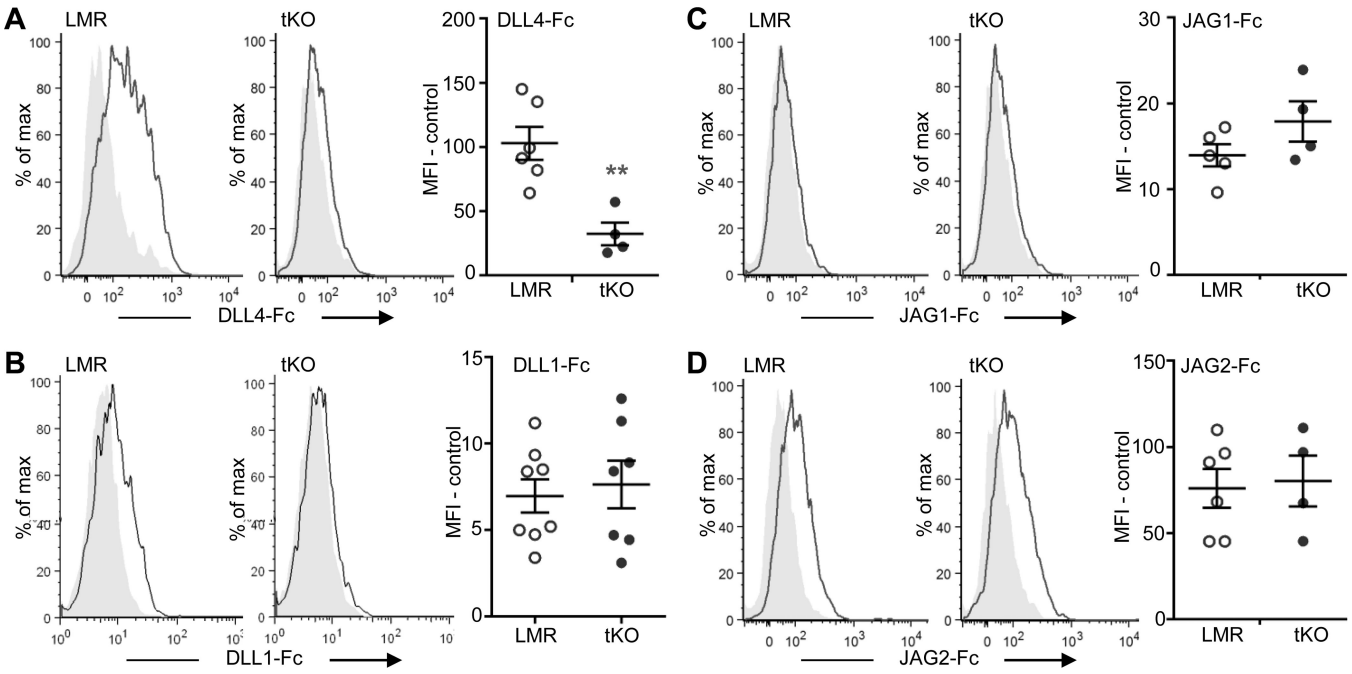

Figure 1.

Notch ligand binding in *Fng* tKO DN T cell progenitors. (**A**) Representative flow cytometry profiles of DLL4-Fc binding to fixed DN T cell progenitors from *Fng* LMR and *Fng* tKO cells. Gray profile is anti-Fc control, solid line is DLL4-Fc binding. Scatter plot shows mean fluorescence index (MFI) ± SEM. MFI for anti-Fc Ab was subtracted from MFI for DLL4-Fc (MFI-control). Symbols reflect the number of *Fng* LMR (open circles) and *Fng* tKO mice (closed circles) from one experiment. Fixed cells had been stored for up to 3 months at 4°C. Relative *Fng* LMR:tKO binding levels were similar in a separate cohort of 4 *Fng* LMR and 3 *Fng* tKO mice in two independent experiments. ***p* <0.005. (**B**) As in (A) but for DLL1-Fc. (**C**) As in (A) but for JAG1-Fc. (**D**) As in (A) but for JAG2-Fc.

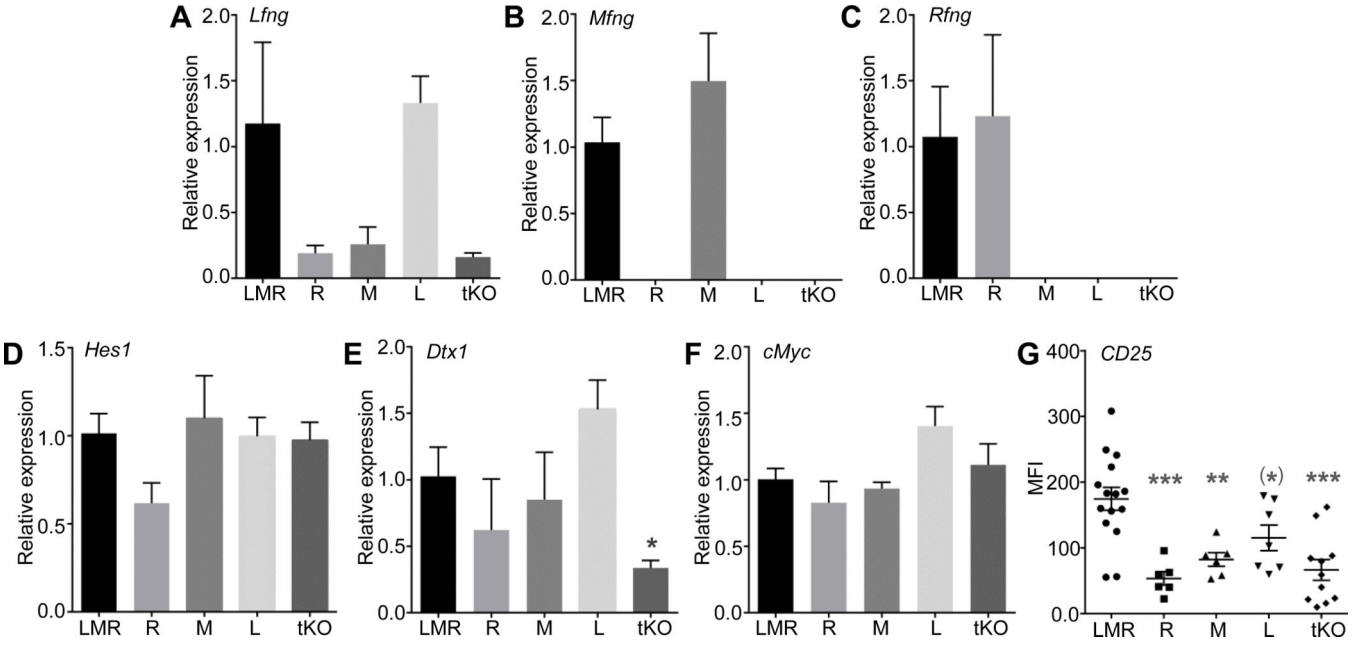

Figure 2.

Fringe and Notch target gene expression in DN T cell progenitors. Transcripts from DN T cell progenitors of *Fng* LMR and *Fng* dKO or tKO mutant mice were converted to cDNA and subjected to qRT-PCR as described in Materials and Methods. The *Fng* gene(s) expressed in each mouse group are given in single letter code (L, *Lfng*; M, *Mfng*; R, *Rfng*). Data reflect a single experiment performed in triplicate for each primer set. (A) *Lfng*, (B) *Mfng*, (C) *Rfng*, (D) *Hes1*, (E) *Dtx1* and (F) cMyc. An independent experiment performed in triplicate on the same cDNA samples gave equivalent results. Independent experiments on a different mouse cohort also gave similar results (see Results). Relative expression was determined based on the average deltaCt obtained for *Actb*, *Gapdh* and *Hprt* combined. Histograms reflect mean and range for *Fng* LMR mice (n=2) and mean ± SEM for mutant mice (n=3). **p*<0.05 based on the two-tailed Student's *t* test. (G) CD25 expression in DN T cells. After gating on CD4−CD8− thymocytes, MFI was determined for CD25 in *Fng* LMR, R, M, L and tKO DN T cells. Scatter plots show mean fluorescence index (MFI) ± SEM. Significant differences from *Fng* LMR, ***p* <0.01, *** *p* <0.001 based on the two-tailed Student's *t* test; (*) *p*<0.05 based on the one-tailed Student's t test.

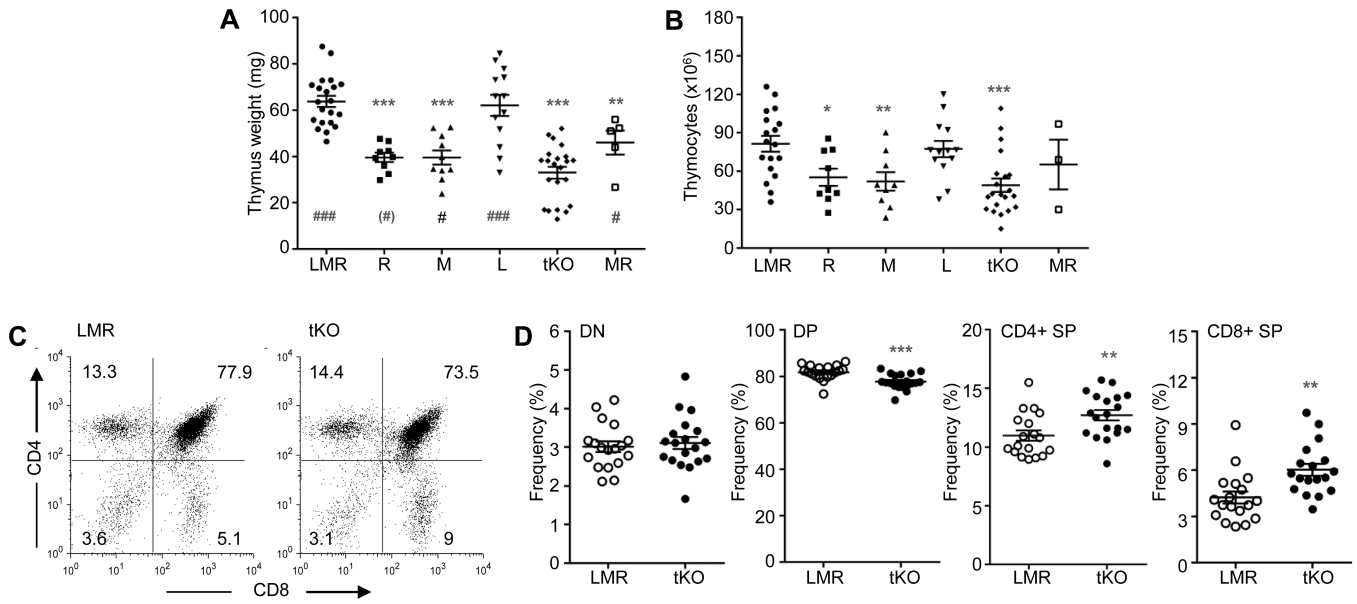

Figure 3.

Thymus and T cell development in *Fng* mutant mice. (**A**) Thymus weight in control *Fng* LMR and *Fng* mutant mice of 7–8 weeks. (**B**) Thymocytes prepared from the thymi weighed in (A) were counted. The *Fng* gene(s) expressed by each mutant group are given in single letter code (L, *Lfng*; M, *Mfng*; R, *Rfng*). Each symbol in scatter plots represents one mouse analyzed at 7–8 weeks. Statistical comparisons between *Fng* LMR and *Fng* mutants were determined by two-tailed Student's *t* test **p*<0.05, ***p*<0.01, ****p*<0.001. Comparisons between *Fng* tKO and other groups are denoted $^{\#}p$<0.05, $^{\#\#}p$<0.01, $^{\#\#\#}p$<0.001. (**C**) Representative flow cytometry analysis of fresh thymocytes from control and *Fng* tKO mice using antibodies to CD4 and CD8a after gating for 7-AAD-negative cells. Percentage of each T cell subset is shown. (**D**) Frequency of DN T cell progenitors, DP T cell precursors, and SP T cells. ***p* <0.01, ****p* <0.001 based on the two-tailed Student's *t* test.

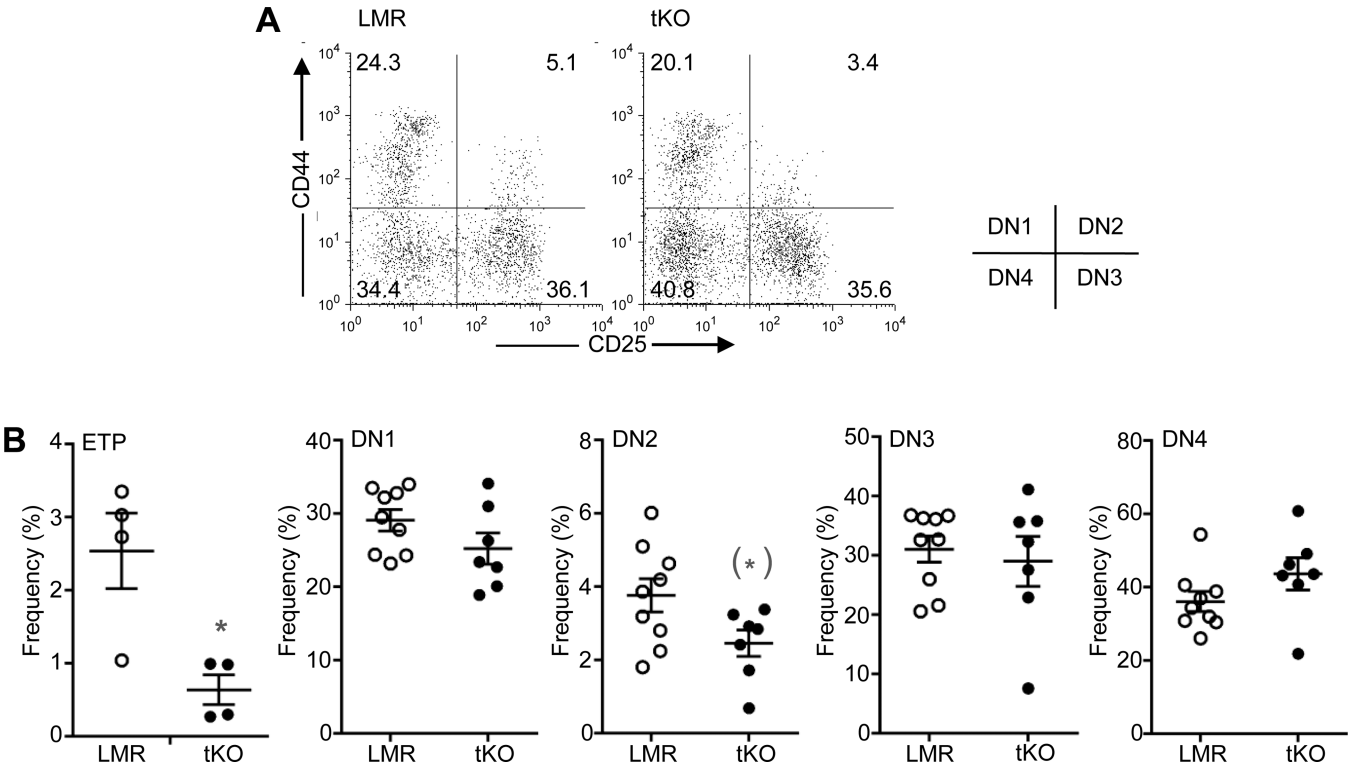

Figure 4.

T cell progenitor subsets in *Fng* LMR and *Fng* tKO thymus. (**A**) Representative flow cytometric analysis using antibodies to CD44 and CD25 after gating on DN T cell progenitors in fresh, 7-AAD-negative thymocytes. Percentages of $CD44^{+}CD25^{-}$ (DN1), $CD44^{+}CD25^{+}$ (DN2), $CD44^{-}CD25^{+}$ (DN3) and $CD44^{-}CD25^{-}$ (DN4) T cell progenitors are indicated. (**B**) Percentage of ETP (DN1 cells that were cKit/CD117+), DN1, DN2, DN3, and DN4 T cell progenitors amongst thymocytes. Mean MFI ± SEM, Each symbol represents a mouse of 7–8 weeks. * $p<0.05$ based on the two-tailed Student's *t* test. (*) $p<0.05$ based on the one-tailed Student's *t* test.

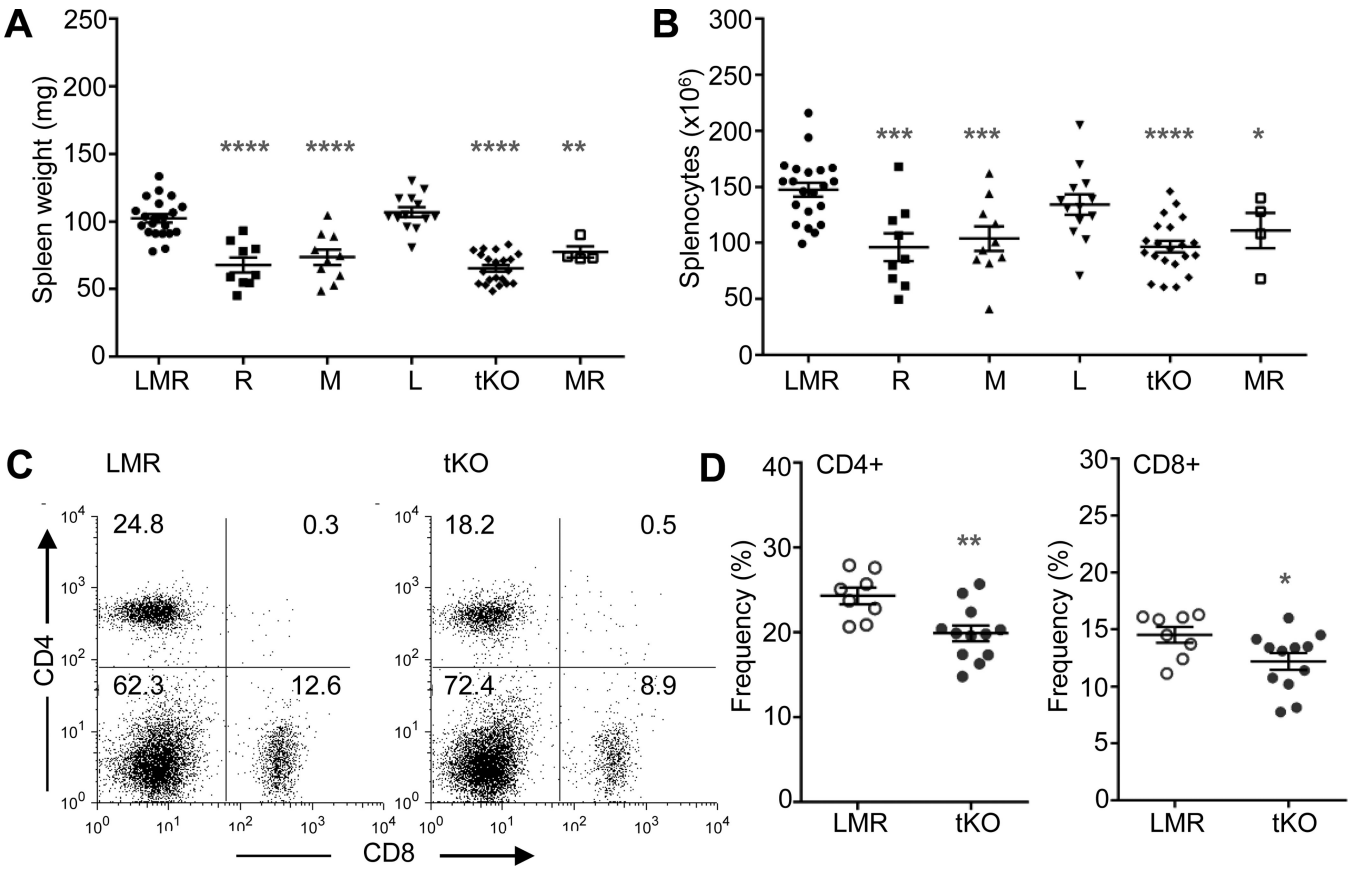

Figure 5.

T cells in spleen of *Fng* LMR and *Fng* mutant mice. (**A**) Spleen weight in *Fng* LMR and *Fng* mutant mice at 7–8 weeks. (**B**) Splenocytes prepared after spleens weighed in (A) were counted. (**C**) Representative flow cytometry analysis of fresh splenocytes from control and *Fng* tKO mice using antibodies to CD4 and CD8a after gating for 7-AAD-negative cells. Percentages of T cell subsets are shown. (**D**) Percentage of $CD4^+$ and $CD8^+$ T cells in splenocytes from *Fng* tKO versus control mice. Mean ± SEM, each symbol represents a mouse. **p* <0.05, ***p* <0.01, ****p* <0.001 based on the two-tailed Student's *t* test.

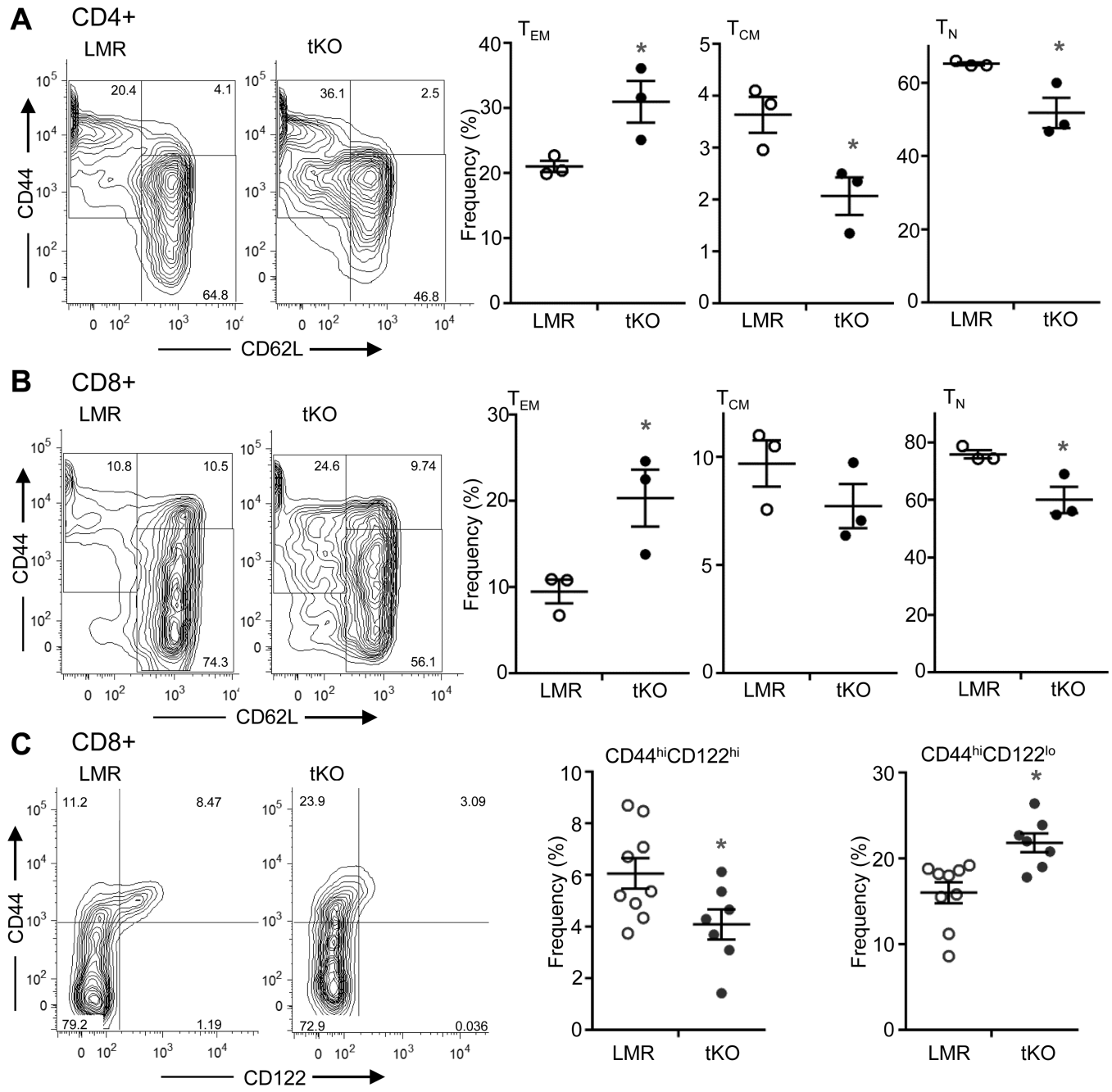

Figure 6.

Effector and memory T cell frequencies in *Fng* tKO spleen. Fresh splenocytes from *Fng* LMR and *Fng* tKO mice of 6–7 weeks were incubated with Abs to CD4, CD8a, CD44 and CD62L and analyzed by flow cytometry. (**A**) Representative profiles of $CD4^+$ effector memory (T_{EM}; $CD44^{hi}CD62L^{lo}$), central memory (T_{CM}; $CD44^{hi}CD62L^{hi}$), and naïve (T_N; $CD44^{lo}CD62L^{hi}$) T cell subsets. Scatter plots give mean ± SEM . **p* <0.05. (**B**) Same as in (A) but gated on $CD8^+$ T cells. (**C**) Expression of CD44 and CD122 in fixed $CD8^+$ T cells from *Fng* LMR and *Fng* tKO splenocytes stored at 4°C for up to 7 months.

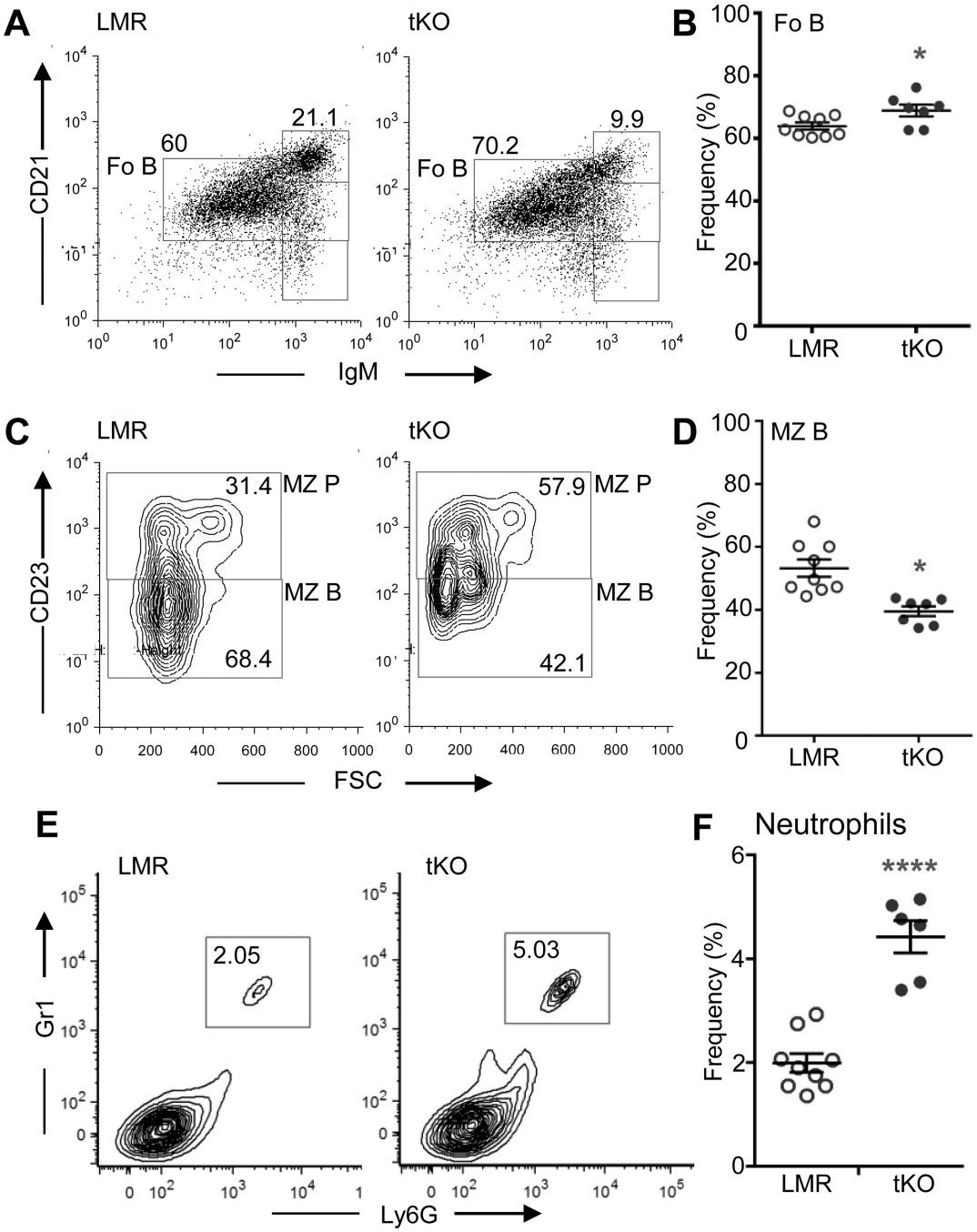

Figure 7.

B cell development in spleen from *Fng* LMR and *Fng* tKO mice. (**A**) Representative flow cytometric analysis of B cell subsets of *Fng* tKO and control mice of 6–7 weeks using antibodies to B220, IgM, CD21 and CD23. B cell subsets were defined based on IgM versus CD21 expression after gating on 7-AAD-negative $B220^{+}$ cells, as shown in the flow cytometry profiles. Fo B cells were $IgM^{int/lo}CD21^{int}$. The $IgM^{hi}CD21^{hi}$ subset was further subdivided into MZ P and MZ B cells based on FSC and CD23 expression, as shown in (**C**). Percentages of Fo B (**B**) and MZ B (**D**) cells in 7-AAD-negative $B220^{+}$ splenocytes from

Fng tKO mice and control mice are shown. Mean ± SEM, **p* <0.05 based on the two-tailed Student's *t* test. (**E**) Fixed splenocytes stored at 4°C for up to 7 months from *Fng* tKO and control mice of 6–7 weeks were incubated with Gr1 and Ly6G antibodies and the frequency of neutrophils (Gr1+Ly6G+) was determined by flow cytometry. (**F**) Percentage of neutrophils in splenocytes from *Fng* tKO mice and control mice. Mean ± SEM, ****p < 0.0001 based on the two-tailed Student's *t* test.

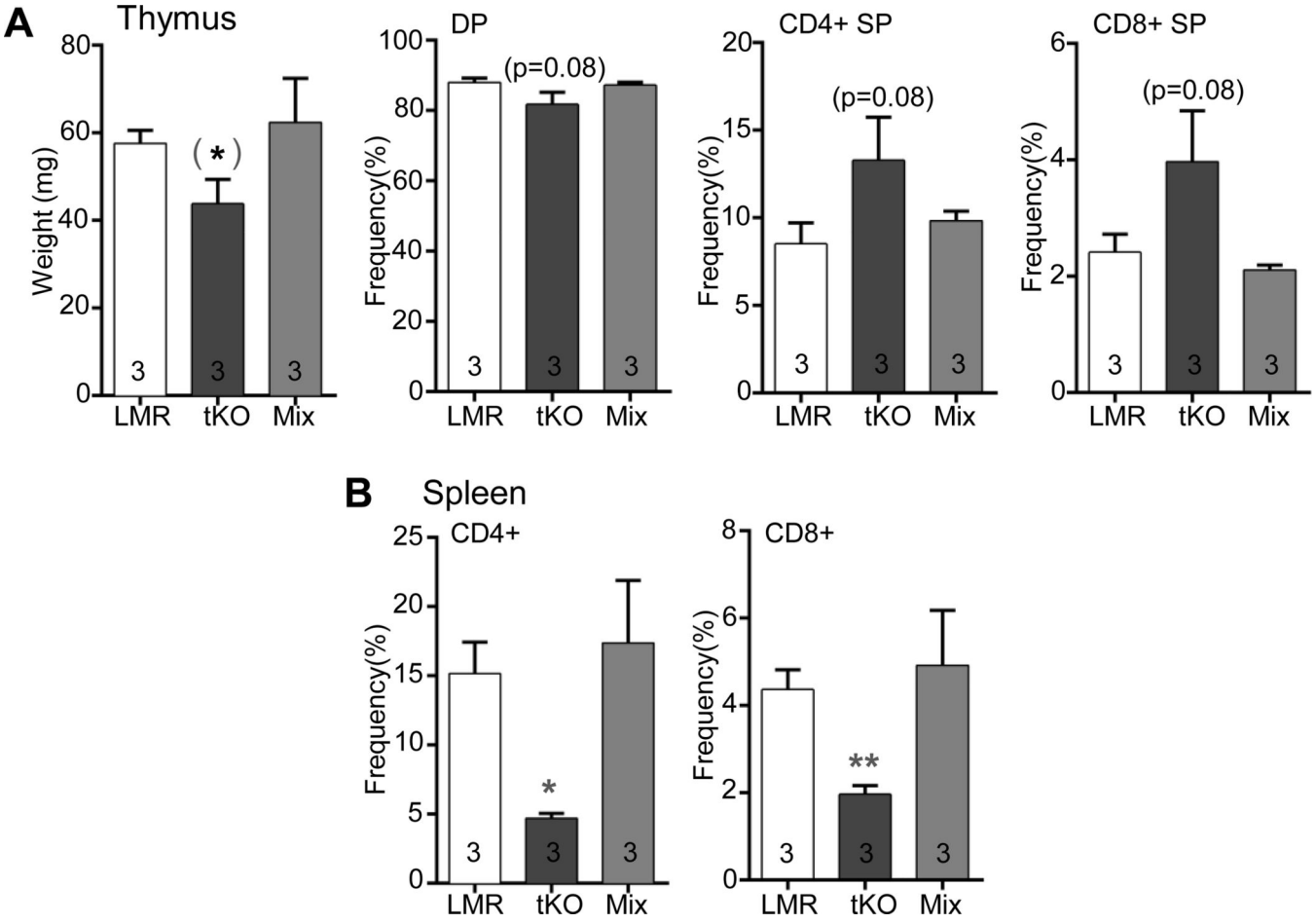

Figure 8.

The *Fng* tKO phenotype is transferable. (**A**) Thymus weight and percentages of DP T cell precursors and CD4+ and CD8+ SP T cells of donor origin in mice of 6 weeks that received 3×10^6 *Fng* LMR, or *Fng* tKO, or a 1:1 mix of *Fng* LMR + *Fng* tKO bone marrow. Mean ± SEM from 3 recipients per group. (*) $p < 0.05$ and $p = 0.08$ based on the one-tailed Student's *t* test. The average donor contribution was 58% (*Fng* LMR), 80% (*Fng* tKO), 88% (mix). (**B**) CD4+ and CD8+ T cells of donor origin from spleen of 3 recipient mice. Mean ± SEM, $*p < 0.05$, $**p < 0.01$ based on the two-tailed Student's *t* test. The average donor contribution was 76% (*Fng* LMR), 69% (*Fng* tKO), or 73% (mix).

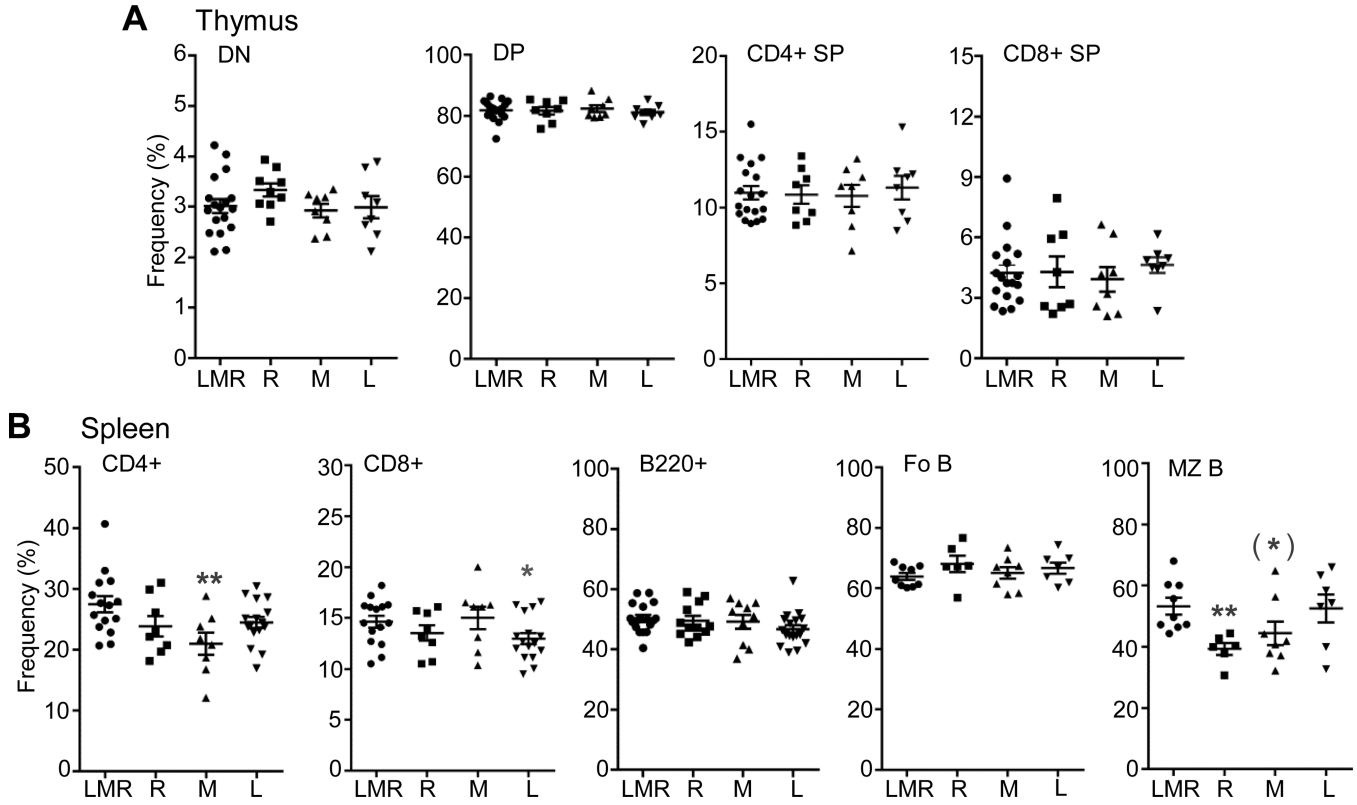

Figure 9.

Individual *Fng* genes support T and B cell development in thymus and spleen. (**A**) Frequencies of DN T cell progenitors, DP T cell precursors, and CD4+ and CD8+ SP T cells were determined for 7-AAD-negative thymocytes from *Fng* LMR mice and mice of 7–8 weeks expressing a single *Fng* gene (L, M or R). (**B**) Frequencies of 7-AAD-negative $CD4^+$ and $CD8^+$ T cells and B220+ B cells in splenocytes from *Fng* LMR mice and mice expressing a single *Fng* gene. Frequency of Fo B cells amongst 7-AAD-negative B220+ splenocytes and of MZ B cells amongst Fo B cells determined as shown in Fig. 7. Mean ± SEM; **p* <0.05, ***p* <0.01 based on the two-tailed Student's *t* test; (*) $p < 0.05$ based on the one-tailed Student's *t* test.

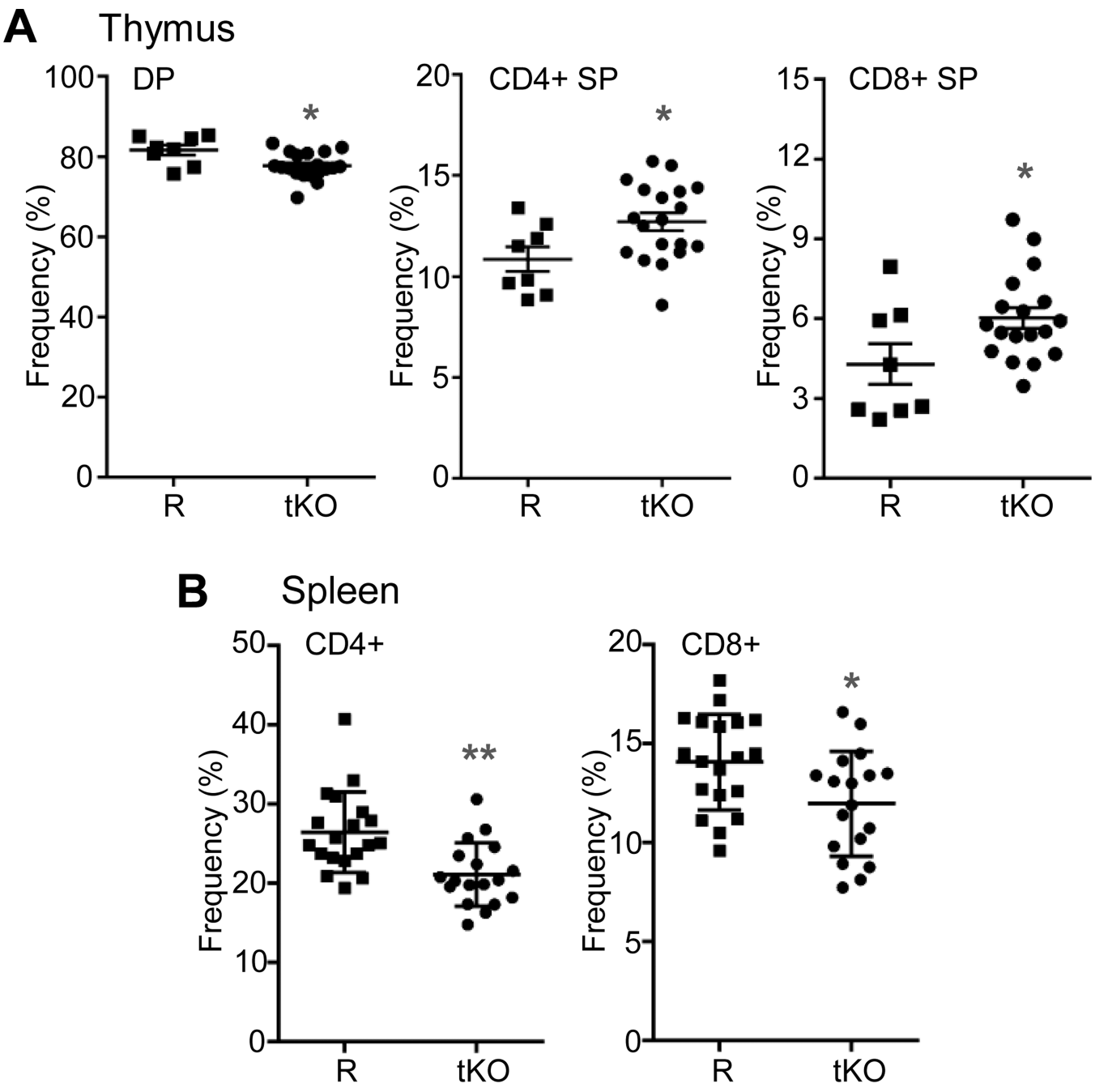

Figure 10.

Rfng contributes to T cell development. (**A**) Frequencies of DP T cell precursors and SP T cells in 7-AAD-negative thymocytes of mice of 7–8 weeks expressing a single allele of *Rfng* (R) versus *Fng* tKO mice. (**B**) Percentage of 7-AAD-negative CD4+ and CD8+ T cells in splenocytes of mice expressing only *Rfng* versus *Fng* tKO mice. Each symbol represents a mouse. Mean ± SEM. **p* < 0.05, ***p* < 0.01 based on the two-tailed Student's *t* test.

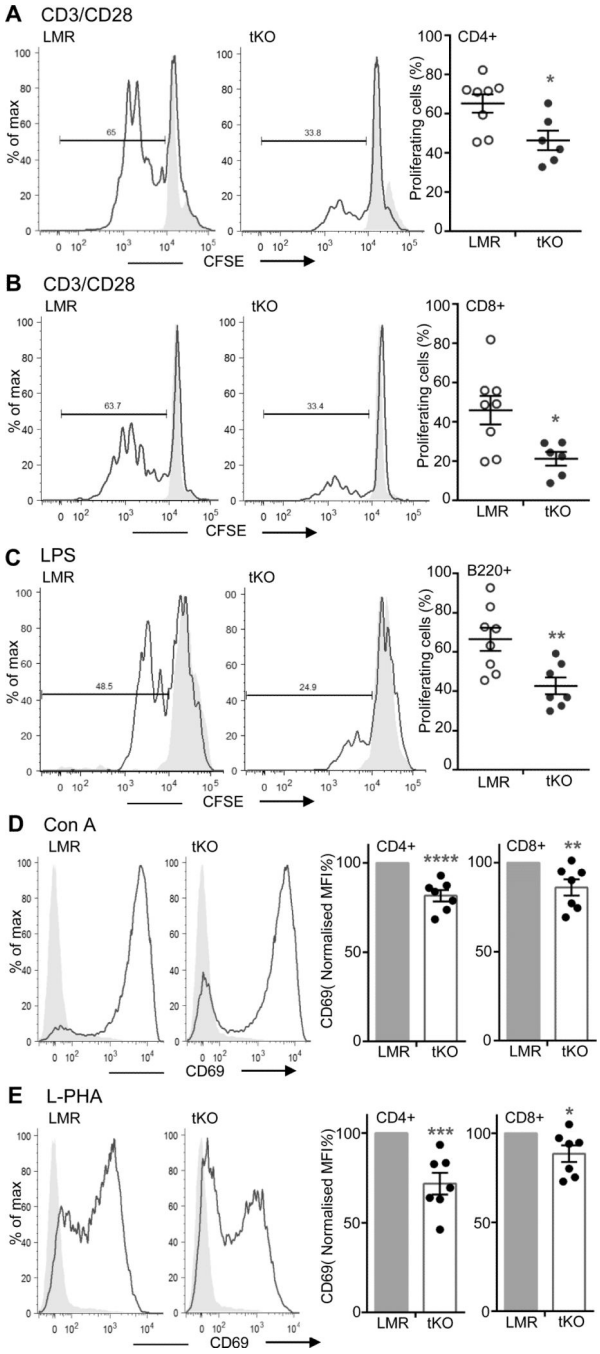

Figure 11.

Impaired proliferation and activation of splenocytes from *Fng* tKO mice. Splenocytes from *Fng* LMR or *Fng* tKO mice of 6–7 weeks were labeled with CFSE and stimulated with anti-CD3/CD28 Dynabeads and IL-2, or LPS as described in Materials and Methods. After 3 days, cells were analyzed for CFSE in 7-AAD-negative $CD4^+$ and $CD8^+$ T cells or B220+ B cells by flow cytometry. Representative flow cytometric analyses of CFSE in (**A**) $CD4^+$ T cells, (**B**) CD8+ T cells or (**C**) B220+ B cells. Unstimulated cells are represented by the gray profile, scatter plots show the average percentage of proliferating T cells in splenocytes from

each mouse, and are the combined data from 4 independent experiments performed in duplicate. Values are mean ± SEM. *$p < 0.05$, **$p < 0.01$ based on the two-tailed Student's *t* test. (**D**) Con A (5 μg/ml) or (**E**) L-PHA (2 μg/ml) were used to stimulate splenocytes from the same *Fng* LMR or *Fng* tKO mice for 20 h. Cells were analyzed for 7-AAD-negative CD69 expression on $CD4^+$ and $CD8^+$ T cells by flow cytometry. Unstimulated cells are represented by gray profiles. Scatter plots represent MFI normalized to control (100%) combined from 4 independent experiments performed in duplicate as in (A). *Fng* LMR MFI values ± SEM were Con A/CD4+ 9226 ± 1759; Con A/CD8+ 8617 ± 1713; L-PHA/CD4+ 1547 ± 304; L-PHA/CD8+ 2933 ± 599. Values for *Fng* tKO are mean ± SEM. *$p < 0.05$, **$p < 0.01$, ***p < 0.0005, ****p < 0.0001 based on the two-tailed Student's *t* test.

Table 1

Notch Ligand Binding to DN T Cell Progenitors

***Fng* Gene(s) Expressed**	**DLL1-Fc MFI-control (no. mice)**	**DLL4-Fc MFI-control (no. mice)**
Lfng, *Mfng*, *Rfng*	5.2 ± 1.1 (n=11)	25.6 ± 1.6 (n=17)
Mfng only	6.1 ± 2.1 (n=5)	15.5 ± 4.2 (n=7)*
Rfng only	5.3 ± 3.2 (n=3)	17.6 ± 7.0 (n=3)
No *Fng*	4.4 ± 1.4 (n=12)	10.0 ± 1.9 (n=14)***

Notch ligand binding to fixed DN T cells stored at 4°C for up to 12 days was assessed by flow cytometry. Mean MFI-control values ± SEM are given for DLL1-Fc and DLL4-Fc used at 500 ng per 3×10^6 cells. Significance was determined by comparing *Fng* LMR to each mutant cohort by two-tailed Student's *t* test.

* $p < 0.05$

*** $p < 0.001$.